

# Towards the field binary population: Influence of orbital decay on close binaries

C. Korntreff<sup>1</sup>, T. Kaczmarek<sup>2</sup>, and S. Pfalzner<sup>2</sup>

<sup>1</sup>Jülich Supercomputing Centre, Forschungszentrum Jülich GmbH, 52425 Jülich, Germany

<sup>2</sup>Max-Planck-Institut für Radioastronomie, Auf dem Hügel 69, 53121 Bonn, Germany  
e-mail: t.kaczmarek@mpi-fr-bonn.mpg.de

## ABSTRACT

*Context.* Surveys of the binary populations in the solar neighbourhood have shown that the periods of G- and M-type stars are *log-normally* distributed in the range from 0.1 – 10<sup>11</sup> days. However, observations of young binary populations in various star forming regions suggest a *log-uniform* distribution. Clearly some process(es) must be responsible for this change of the period distribution over time. Most stars form in star clusters, so it is here that the(se) process(es) take place.

*Aims.* In dense young clusters two important dynamical processes occur: i) the gas-induced orbital decay of embedded binary systems and ii) the destruction of soft binaries in three-body interactions. The emphasis in this work is on orbital decay as its influence on the binary distribution in clustered environments has been largely neglected so far.

*Methods.* We performed Monte-Carlo simulations of binary populations to model the process of orbital decay due to friction with the gas. In addition, the destruction of soft binaries in young dense star clusters was simulated using nbody modelling of binary populations.

*Results.* It is known that the cluster dynamics destroys the number of wide binaries, but leaves short-period binaries basically undisturbed. Here it is demonstrated that this result is also valid for an initially log-uniform period binary distribution. By contrast the process of orbital decay significantly reduces the number and changes the properties of short-period binaries, but leaves wide binaries largely unaffected. Until now it was unclear whether the short period distribution of the field is unaltered since its formation. It is shown here, that if any alteration took place, then orbital decay is a prime candidate for this task. In combination the dynamics of these two processes, convert even an initial log-uniform distribution to a log-normal period distribution. The probability is 94% that the evolved period distribution and the observed period distribution have been sampled from the same parent distribution.

*Conclusions.* Our results provide a new picture for the development of the field binary population: Binaries can be formed as a result of the star-formation process in star clusters with periods that are sampled from the log-uniform distribution. As the cluster evolves, short-period binaries are merged to single stars by the gas-induced orbital decay while the dynamical evolution in the cluster destroys wide binaries. The combination of these two equally important processes reshapes a initial log-uniform period distribution to the log-normal period distribution, that is observed in the field.

**Key words.** Keywords should be given

## 1. Introduction

The most important observations that shaped our current picture of the binary field population were already performed in the early 1990's. Duquennoy & Mayor (1991) determined the binary frequency of G-type stars in the solar neighbourhood to be about 61% and the period distribution to follow a log-normal distribution,

$$f(\log P) = C \exp \left\{ \frac{-(\log P - \overline{\log P})^2}{2\sigma_{\log P}^2} \right\}, \quad (1)$$

over the period range  $\sim 10^{-1} - 10^{11}$  d where P is the period in days ( $\overline{\log P} = 4.8 \equiv 172$ yr,  $\sigma_{\log P} = 2.3$ ) and C a normalisation constant. A year later Fischer & Marcy (1992) analysed the binary properties of M-dwarfs in the separation range 0.04–10<sup>4</sup> AU corresponding to periods in the range  $\sim 10^{-2} - 10^6$ yr and found that the period distribution of M-dwarfs in the solar neighbourhood is also log-normally distributed with a peak between 9yr and 270yr - nearly identical to the findings for the G-dwarfs. Although the observed binary frequency of M-dwarfs with about 33% is lower than that of G-dwarfs, the properties of the G and M-dwarf binary populations seem very similar. More recent ob-

servations by Raghavan et al. (2010) confirm this picture. They determined the binary properties of nearby ( $d < 25$ pc) solar-type stars ( $\sim F6 - K3$ ) and find the fraction of binary stars to be 58% with a log-normal period distribution ( $\log P = 5.03$  and  $\sigma_{\log P} = 2.28$ ).

With an average age of a few Gyrs the field population constitutes a dynamically evolved state. Therefore, dynamical processes have most likely changed the binary properties since the formation of these stars and the current properties differ significantly from the primordial state. In order to understand the binary formation process it is not sufficient to know the properties of the (old) field population but those of the primordial binary population.

Connelley et al. (2008) determined the binary properties of the very young populations in Taurus, Ophiuchus and the Orion star-forming regions (excluding the much denser Orion Nebula Cluster). They found that their observed period distribution can be fitted by a log-uniform distribution, differing significantly from the log-normal distribution in the field (see also Kraus & Hillenbrand (2007)). In these sparse young star forming regions it is improbable that dynamical evolution altered the period distributions in the short period since the stars were formed (see

e.g. Kroupa & Bouvier 2003). So it can be assumed that their properties match the initial conditions in general.

In denser regions indications for an originally log-uniform distribution are found, too. For example, HST observations by Reipurth et al. (2007) of binaries in the Orion Nebula Cluster (ONC) demonstrate, that the semi-major axis distribution deviates from the log-normal distribution and is closer to a log-uniform distribution. So it seems that older binary populations have a *log-normal* period distribution while the primordial distribution is likely to be *log-uniform*.

From the theoretical side the binary frequency is the best studied binary property (e.g. Kroupa & Burkert 2001; Kroupa & Bouvier 2003; Kroupa et al. 2001; Pfalzner & Olczak 2007; Marks et al. 2011; Marks & Kroupa 2011). It seems that also the evolution of the binary frequency in the ONC depends on the initial binary frequency, the evolution of the binary population does not (Kaczmarek et al. 2011). However, the binary population is not only described by the binary frequency but also by the period, mass-ratio and eccentricity distribution.

Starting with the work by Heggie (1975), it has been realised that binaries become dynamically destructed via three- and four-body interactions. Generally wide binaries are more affected by dynamical destruction than close ones. The existence of binaries wider than  $10^3$  AU in the field still poses an open question regarding their origin (Parker et al. 2009).

Performing N-body simulations Kroupa (1995a,b) showed, that to reproduce the observed log-normal distribution of the field, the initial number of wide binaries has to be significantly higher than observed, if all binaries are exposed to dynamical evolution in a star cluster. This rising distribution was obtained by inverse dynamical population synthesis, inverting the effects of dynamical destruction on the period distribution (see dashed line in Fig. 1).

Parker et al. (2009) finds that binaries with periods exceeding  $10^3$  AU cannot survive in these clusters he investigated. However, binaries with semi-major axes exceeding  $10^3$  AU are observed in the field. Kouwenhoven et al. (2010) suggest, that these observed wide binaries could form during the cluster dissolution. Another approach would be a different cluster type.

Here we investigate how the initial period distribution would evolve in its natal environment considering the two different dynamical processes that inevitably affect binaries in a cluster: i) gas-induced orbital decay and ii) dynamical destruction of binaries in encounters.

So far the influence of orbital decay has been only investigated for isolated binary systems Stahler (2010). Orbital decay takes place in the earliest stages of star formation, when the stars are still embedded in the gas. Here the interaction of binaries with the gas leads to the excitation of waves in the surrounding gas. The energy transfer from the binary to the gas leads to orbital decay (Stahler 2010). Here we investigated how orbital decay changes the period distribution in a cluster environment.

This paper is structured in the following way: in Section 2 the cluster setup is explained. Section 3 describes the orbital decay process in the gas embedded phase. We demonstrate in Section 4 that a combination of the orbital decay with the dynamical destruction (Kaczmarek et al. 2011) naturally transforms a log-normal birth period distribution into a log-uniform period distribution. Our conclusions mark the last section.

## 2. Cluster Setup

The processes of orbital decay and dynamical destruction take inevitably place as soon as the binary population forms in a

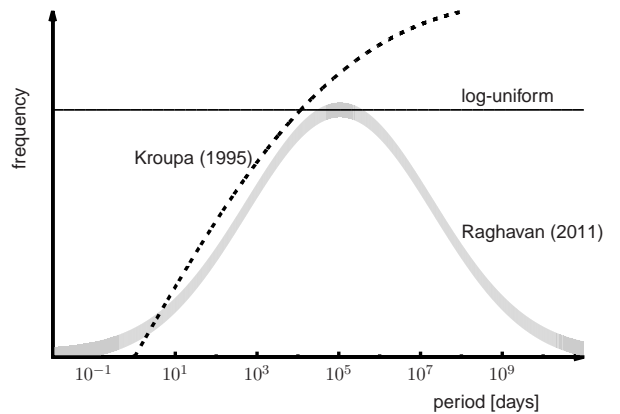


**Fig. 1.** Schematic picture of possible initial period distributions. The thick grey curve displays the log-normal fit to the data of Raghavan et al. (2010), the thick dashed line the Kroupa (1995a) and the solid line a log-uniform period distribution, that is observed in many young star forming regions (see text for references).

dense star cluster environment. Both result from interactions between stars in a dense environment. As most stars form in cluster environments (Lada & Lada 2003), it can be anticipated that the field binary population we observe today was - at least to some extent - shaped by these processes.

In this study we chose the Orion Nebula Cluster (ONC) as model cluster. It is probably a typical star forming region and has the advantage that many parameters both of the cluster structure and the binary population are well observed (e.g. Jones & Walker 1988; Prosser et al. 1994; Hillenbrand 1997; Hillenbrand & Hartmann 1998; O'Dell et al. 2009; Preibisch et al. 1999; Köhler et al. 2006; Reipurth et al. 2007). The radial density profile declines in the outer parts as  $\rho_{\text{present}} \propto r^{-2}$  (Jones & Walker 1988; Hillenbrand 1997) and is much flatter ( $\rho_{\text{core}} \propto r^{-0.5}$ ) within  $R_{\text{core}} \approx 0.2$  pc. The dynamical evolution of the cluster significantly changes the stellar density profile during the first Myr, the estimated age of the ONC (Hillenbrand 1997). Hence we adopted the following initial density profile

$$\rho_{\text{star}}(r) \propto \begin{cases} (r/R_{\text{core}})^{-2.3}, & 0 < r \leq R_{\text{core}} \\ (r/R_{\text{core}})^{-2.0}, & R_{\text{core}} < r \leq R \\ 0, & R < r \leq \infty. \end{cases} \quad (2)$$

Here we choose  $R_{\text{core}} = 0.2$  pc and a cluster size of  $R = 2.5$  pc to model the ONC. The used model starts from a situation where all stars are already formed. In dynamical equilibrium the initial radial density profile (Eq. 2) evolves towards the currently observed one over a time span of about 1 Myr (Olczak et al. 2010). However, other initial conditions could result in the same profile (Kroupa 2000; Allison et al. 2009).

To mimic the often observed mass-segregation in young dense clusters, the most massive binary system is initially placed at the cluster centre and the three next most massive stars at random positions within a sphere of radius  $R = 0.6 R_{\text{hm}}$  around the cluster centre, where  $R_{\text{hm}}$  is the cluster half-mass radius. In this we follow the suggestions by Bonnell & Davies (1998), who found that the observed mass segregation (Hillenbrand & Hartmann 1998) of the ONC is unlikely to be the result of the dynamical evolution of the cluster but has to be primordial, if the cluster is initially in virial equilibrium. Note, that if the cluster would be in a subvirial state, probably no primordial mass

segregation would be required (Allison et al. 2009; Olczak et al. 2011).

All stellar systems are initially created as binaries with system masses sampled from the initial mass function (IMF) suggested by Kroupa (2007, Eqs. 19 & 20). We limited our system mass  $M_{\text{sys}} = M_{s1} + M_{s2}$  to  $[0.08 M_{\odot}, 50 M_{\odot}]$ , where  $M_{s1}$  and  $M_{s2}$  are the masses of the stars constituting a binary system. The upper mass limit corresponds to the mass of the most massive binary system of the ONC. The lower limit is the hydrogen burning limit, and thus the margin between sub-stellar and stellar objects.

Ideally we would like to use observed initial properties of binaries in very young embedded clusters. We will see that embedded clusters younger than 100,000 yr would be ideal, because at such a young age the binary population would be close to its primordial state. However, it is very difficult to observe clusters at such a young age. Observations of binaries in dense embedded clusters face a number of observational difficulties like extinction, crowding, resolution etc.. In addition, the number of stars would be very low, making statistical statements impossible. As there is an age spread in forming clusters (1-3 Myr) it would be a possibility to use just the youngest stars in a forming cluster to deduce the primordial state. However, age determination for such young stars is problematic. Alternatively, one can assume that low density clusters are relatively unaffected by these processes described here and are therefore close to their primordial state. Observations of the primordial state not being available, we use the work by Kouwenhoven et al. (2007) based on observations of the low-density Scorpius OBII cluster. Choosing the semi-major axis and mass ratio distribution from an OB association with an age of (5-20) Myrs (Kouwenhoven et al. 2007), as Scorpius OBII, seems at first glance unusual, as at that age the binary population might have already been processed. However, the low stellar density of Scorpius OBII combined with the lack of surrounding gas speaks for the cluster having neither been processed by orbital decay nor by dynamical destruction, as mentioned before.

The primordial semi-major axis distribution was chosen to be log-uniform  $f_a(a) \propto dN/da \propto a^{-1}$  with  $a \in [0.02 \text{ AU}, 10000 \text{ AU}]$ . As primordial mass ratio distribution we started with  $f_q(q) \propto q^{0.4}$  and  $q = M_{s2}/M_{s1} \in [0, 1]$ .

Another justification for our choice of the initial semi-major axis distribution, is that the log-uniform distribution is a simple straight forward distribution, that requires strong processing in order to obtain the log-normal field distribution. This distribution was used here to test, if even this extreme assumption leads to the log-normal distribution observed in the field. This does not rule out, that one obtains a similar result as described in the following with different initial conditions, containing fewer wide and/or close binaries.

In the following the above described model will be used to study the effect of the gas-induced orbital decay of binaries in star clusters.

### 3. Gas-induced Orbital Decay

In the early embedded phases clusters consist of the already formed stars and a large gas component from which further stars potentially form. These stars keep being embedded in their natal gas cloud until it is removed by strong winds, radiation of the massive stars and supernova explosions. During this embedded phase, stars and binary systems experience dynamical friction with the ambient gas. Binary systems induce spiral waves in the gas leading to energy and angular momentum loss resulting in a shrinking of the binary orbit and possibly merging of the two

stars. Stahler (2010) derived an analytic expression for the temporal development of the separation  $a_{\text{tot}}$  for a single isolated binary system on a circular orbit. The separation diminishes due to gas-induced orbital decay with time as

$$a_{\text{tot}} = a_0 \left(1 - \frac{t}{t_c}\right), \quad (3)$$

where  $a_0$  is the initial binary separation and  $t_c$  the so-called coalescence time, which is given by

$$t_c = \frac{15}{32\pi} \frac{(1+q)^2}{q} \frac{c_s^5}{\rho_0 G^3 M_{\text{sys}}^2} a_0, \quad (4)$$

where  $G$  is the gravitational constant,  $c_s$  the sound speed,  $q$  the mass ratio and  $M_{\text{sys}}$  the system mass of the binary system.

Stahler (2010) assumed in his derivation that gas interactions close to the stars themselves can be neglected. The binary system, represented by an oscillating gravitational potential, torques the nearby gas and produces outgoing acoustic waves. These waves transport angular momentum from the binary to the surrounding gas. Thus the orbit of the binary decays as long as the gas density is high enough. Eq. 3 is only valid for radial distances

$$a_{\text{tot}} < r^{\text{max}} = \frac{G M_{\text{sys}}^{\text{min}}}{2 c_s^2} = 111 \text{ AU} \left(\frac{M_{\text{sys}}^{\text{min}}}{M_{\odot}}\right) \left(\frac{c_s}{2 \text{ km s}^{-1}}\right)^{-2}, \quad (5)$$

between the two stars constituting the binary system.

To analyse the effect of gas-induced orbital decay of binary systems on the period distribution, we applied Eq. 3 to the entire population of a young star cluster, for the example of the ONC. Starting from a cluster with initial conditions as given in Sec. 2, the temporal development of the binary population is followed for different gas density models.

Only if a binary system fulfills the restriction given by Eq. 5 the orbital decay is calculated, otherwise the orbit remains unaltered. This means, for example, for a system mass of  $0.08 M_{\odot}$ ,  $1 M_{\odot}$  and  $50 M_{\odot}$  the orbital decay will only be calculated for binary systems with a separation  $r < 8.88 \text{ AU}$ ,  $r < 111 \text{ AU}$  and  $r < 5550 \text{ AU}$ . Like in Stahler's work modelling the orbital decay the simplification of treating all orbits as circular has been adopted. Future work should include elliptical orbits as well.

For the gas-induced decay, the gas density distribution in the cluster is of vital importance. Here we assume an isothermal gas density which follows the stellar density distribution. To prevent the distribution from diverging at the centre, the density is kept constant at a value  $\rho_{\text{max}}$  inside the cluster core radius  $R_{\text{core}} = 0.2 \text{ pc}$ . Outside this area the density decreases isothermally. Thus the isothermal gas density distribution can be described by the following equation

$$\rho_{\text{gas}}(r) = \rho_{\text{max}} \begin{cases} 1, & r < R_{\text{core}} \\ (R_{\text{core}}/r)^2, & R_{\text{core}} < r < R_{\text{cluster}} \end{cases} \quad (6)$$

For an isothermal density distribution  $\rho_{\text{gas}}(r) = c_s^2/2\pi G r^2$  (e.g. Binney & Tremaine 1987, Eq. 4.123) the sound speed is given by

$$c_s = \sqrt{2\pi G \rho_{\text{gas}}(r) r^2}. \quad (7)$$

Although the density distribution (Eq. 6) is not isothermal over the whole parameter range, we approximate the sound speed as

$$c_s = \sqrt{2\pi G \rho_{\text{max}} r_{\text{core}}^2}. \quad (8)$$

The resulting sound speeds for distributions with  $\rho_{max} \in [10^4, 10^6] \text{cm}^{-3}$  lie between the sound speed of an ideal gas at 10K,  $c_s = 0.2 \text{km/s}$ , and the observed value in infrared dark clouds (Sridharan et al. 2005)  $c_s = [1.0 - 2.2] \text{km/s}$ . A even better approach would be a time dependent density  $\rho(r, t)$  and sound speed  $c_s(r, t)$ , which hasn't been observed yet. Deviations of the sound speed manifest themselves in the coalescence time (Eq. 4).

If the separation becomes smaller than the radius of both stars  $a_{tot} < R_{s1} + R_{s2}$  (assuming a main-sequence mass-radius relationship (Binney & Merrifield 1998, p. 110)),

$$\left(\frac{R_{s1/2}}{R_{\odot}}\right) \approx \left(\frac{M_{s1/2}}{M_{\odot}}\right)^{0.7},$$

a binary system is treated as a 'merged' system. This is clearly a strong simplification, because the merging of stars is a much more complex process that depends on a variety of parameters such as the presence of a surrounding disc, the eccentricity of the orbit, mass transfer and the conditions of the molecular cloud in which the stars are embedded. However, including all these processes goes beyond the aim of the current paper. Here, all processes at these small distances are excluded under the assumption that these two stars might possibly merge at such small distances.

First it was analysed how the binary population parameters change due to orbital decay in general. Therefore, a series of simulations with three different gas densities in the range of  $[10^4 \text{cm}^{-3}, 10^6 \text{cm}^{-3}]$  were performed corresponding to moderate gas densities observed in star forming regions (Padmanabhan 2001). For the three densities  $10^4 \text{cm}^{-3}$ ,  $10^5 \text{cm}^{-3}$  and  $10^6 \text{cm}^{-3}$  the sound speeds are 0.15 km/s, 0.49 km/s and 1.54 km/s, respectively (Eq. 8). The results summarised in Table 1, show the merger rates for all combinations of gas densities and sound speeds. As to be expected, the percentage of possibly merged binary systems after 1 Myr (Table 1) depends on the maximum density of the isothermal density distribution (Eq. 6). The value of the overall reduction of binaries could vary for a constant sound speed by a factor of two to four if the density would change by one order of magnitude. Keeping the density constant, one can see, that the percentage of merged systems is sensitive to the choice of sound speed.

Additionally, the degree of orbital decay depends on the gas density distribution. Here only the case of a temporary constant and spatially isothermal gas density distribution has been described as this fits best the observed period distribution and seems a realistic assumption for the here studied case of an ONC-type cluster.

In the following an isothermal gas density distribution with  $\rho_{max} = 10^5 \text{cm}^{-3}$  is used for the example of an ONC-like cluster.

sound speed	0.15 km/s	0.49 km/s	1.54 km/s
maximum density			
$10^4 \text{cm}^{-3}$	37.4%	2.8%	0.1%
$10^5 \text{cm}^{-3}$	54.9%	12.0%	0.2%
$10^6 \text{cm}^{-3}$	69.2%	28.7%	1.2%

**Table 1.** Percentage of merged binary systems for different sound speeds and maximum densities after 1 Myr.

In Fig. 2 the number of merged binaries  $N_m$  relative to the initial number of binaries  $N_{tot}$ ,  $\mathcal{N}_m = N_m/N_{tot}$  is plotted as a function of the initial semi-major axis of the merged binary systems. The binaries with small semi-major axis merge to a higher

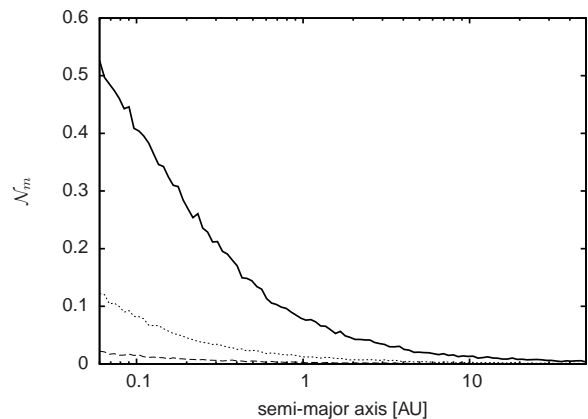


**Fig. 2.** The number of merged binaries relative to the initial number of binaries after 0.01 Myr (dashed), 0.1 Myr (dotted) and 1 Myr (solid) for a binary distribution embedded in an  $r^{-2}$  gas density distribution with  $\rho_{max} = 10^5 \text{cm}^{-3}$  and a sound speed of 0.49 km/s.

degree than wider binaries. Whereas binaries with initial semi-major axis of 10 AU rarely merge, 40% of all binaries with initial semi-major axis of 0.1 AU coalesce after 1 Myr (solid line).

The resulting semi-major axis change depends as well strongly on the system mass  $M_{sys}$ . Figure 3 shows the mean relative semi-major axis change  $\overline{\delta a_0} = [a(0) - a(t)]/a(0)$  as a function of the system mass. This illustrates that the semi-major axis of binaries with a high system mass shrinks faster and to a larger degree than the semi-major axis of binaries of a lower system mass. The shorter coalescence time for massive systems (see Eq. 4) results from the increased angular momentum and energy loss of high-mass binaries due to dynamical friction (Eq. 51 in Stahler (2010)). The average separation between binary systems with  $M_{sys} > 10 M_{\odot}$  dwindles to less than half its initial value after 1 Myr. Additionally, the location of the binary system inside the cluster influences the coalescence time. For a maximum density of  $10^5 \text{cm}^{-3}$  in the cluster core, the density drops to  $6.4 \cdot 10^2 \text{cm}^{-3}$  at 2.5 pc. Therefore the coalescence time of a binary system with  $M_{sys} = 10 M_{\odot}$  drops from 0.23 Myr in the cluster center to 35.95 Myr at 2.5 pc. Considering this, the effect of orbital decay could even boost the mass segregation of the cluster.

The overall effect of the gas-induced orbital decay on the period distribution of the binaries in the cluster is to reshape it by pushing binaries to tighter orbits which can even lead to the merging of a binary. This can be seen in Fig. 4, which shows the relative number of binary systems  $\mathcal{N}_b = N_b(t)/N_b(0)$  as a function of the semi-major axis after 0 Myr (thin solid line), after 0.01 Myr (dashed line), 0.1 Myr (dotted line) and 1 Myr (thick solid line) for a binary distribution embedded in a  $r^{-2}$  gas density distribution with  $\rho_{max} = 10^5 \text{cm}^{-3}$  and a sound speed of 0.49 km/s. Because the orbital decay acts faster for tighter binaries (see. Eq. 4), binaries in the left part of the period semi-major axis distribution are altered first leading to a depopulation of binaries with semi-major axes between 0.02AU and 1AU and the formation of a tail for semi-major axis less than 0.02AU after 0.01Myr. As time goes on, binaries with even larger orbits are affected until the orbital decay process stops when the gas is expelled from the cluster. At this point the process of orbital decay alone is responsible for the binary frequency in the cluster to drop from it's initial value of 100% to 88% through the merging of very tight binaries.

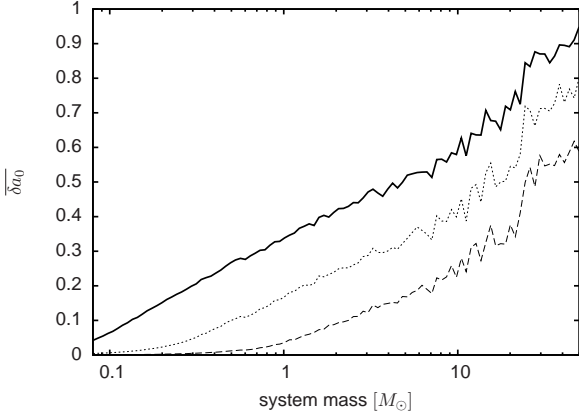


**Fig. 3.** Mean relative semi-major axis change as a function of the system mass for a binary distribution embedded in an  $r^{-2}$  gas density distribution with  $\rho_{max} = 10^5 \text{ cm}^{-3}$  and a sound speed of 0.49 km/s after 0.01 Myr (dashed), 0.1 Myr (dotted) and 1 Myr (solid).

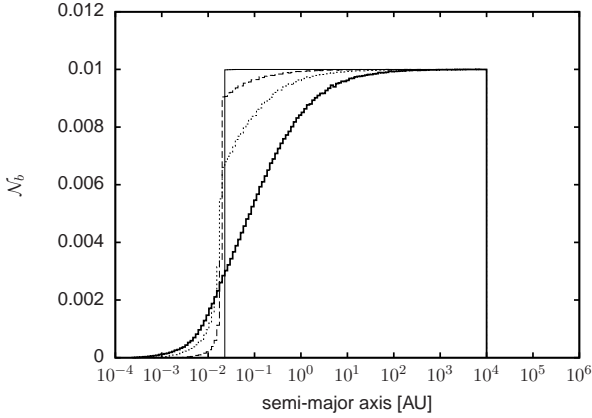


**Fig. 4.** Chosen birth semi-major axis distribution (thin solid line) and effect of the gas induced orbital decay on a semi-major axis distributions embedded in an  $r^{-2}$  gas density distribution with  $\rho_{max} = 10^5 \text{ cm}^{-3}$  and a sound speed of 0.49 km/s after 0.01 Myr (dashed), 0.1 Myr (dotted) and 1 Myr (thick solid).

#### 4. Comparison with observations

In the following we compare above described results with observations. In order to do so, we converted our semi-major axis distributions into period distributions and re-binned our data according to Raghavan et al. (2010). Their observations were limited to F6 to K3 dwarf stars which roughly corresponds to binary systems with primary masses  $M_{s1} \in [0.5 M_{\odot}, 1.5 M_{\odot}]$ .

Figure 5a) shows the resulting initial period distributions as thin solid lines and the final period distributions as thick solid lines for the process of orbital decay. In accordance to the results for the semi-major axis distribution the orbital decay (Sec. 3) reduces the number of short period binaries. In above model the influence of the gas on the binary system has been studied, but the dynamical interactions between the binaries with other stellar components in the cluster were neglected. It is known that dynamical interactions destroy long period binaries. The question arises whether there is any region in the period distribution which is significantly affected by both processes?

To investigate this, we want to show the pure dynamical impact of the cluster evolution on the binary population in absence

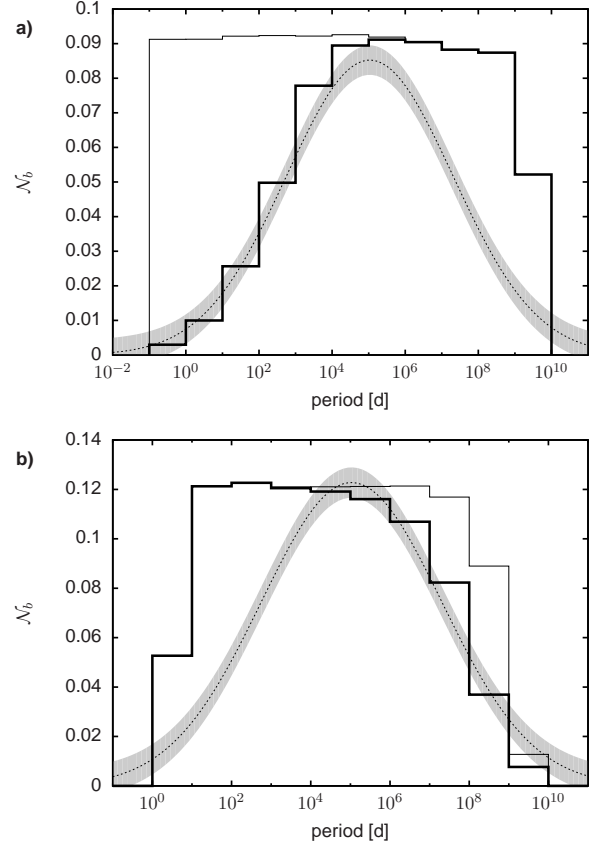


**Fig. 5.** a) Chosen birth period distribution (thin solid line) and effect of the gas induced orbital decay on a period distributions embedded in an  $r^{-2}$  gas density distribution with  $\rho_{max} = 10^5 \text{ cm}^{-3}$  and a sound speed of 0.49 km/s after 1 Myr (thick solid line) compared with the Gaussian fit (dotted line) to the observations by Raghavan et al. (2010). b) Same as in a), with results from the NBODY6 simulations.

of the “gas-effect” described above. So all clusters have been set up without any gas and are initially in virial equilibrium. Only the first 3 Myr are investigated in this study. As only the most massive stars evolve significantly in this time, stellar evolution was not considered in the simulations. To improve statistics, 50 realisations of these clusters have been simulated and their results have been averaged. For more details on the numerical method see Kaczmarek et al. (2011).

To provide comparable initial conditions as in Sec. 3 all simulations have been set up as described in Sec. 2. The formal initial binary frequency has been chosen to be 100% i.e. each star is generated as part of a binary system. However, the resulting initial binary frequency is always lower as a consequence of the setup procedure. All particles in the simulations are created as binaries initially with a semi-major axis sampled from the log-uniform distribution. Afterwards these binaries are placed randomly in the cluster independent of the semi-major axis. Therefore, binaries with separations longer than the local mean separation will often have a closer partner already, so that thereby are fewer large-separation binaries than expected from the set up.

Figure 5b) shows the period distribution of the simulated cluster initially (thin solid line) and at the age of 3 Myr (solid line) with the Gaussian fit (dotted line) to the observations. It can be seen that dynamical evolution of the binary population



in a star cluster mainly destroys wide binaries, but does not affect tight binaries. These wide binaries are destroyed in three- and four-body encounters where a perturber transfers some of its kinetic energy to the binary system so that after the interaction, the binding energy of the binary becomes positive (Heggie 1975). However, this process is only effective if the binary is not too strongly bound which implies that predominantly wide binaries are affected. Nevertheless, after 3 Myr still a small amount of wide binaries exists. Our results give no definite answer to the origin of these wide binaries. They are either remainders of the initial binary population or formed by dynamical processes. The reason is that also we perform a large number of simulations the results for the wide binaries still suffer from low number statistics.

Similar results were obtained by e.g. Kroupa (1995a); Kroupa et al. (2001) using a initial period distributions with a higher number of initial wide binaries than used here (dashed line in Fig. 1). It should be noted that, using a log-normal distribution with a initial lower number of wide binaries (thick grey line in Fig. 1) Parker et al. (2009) obtained a deficiency of wide binaries in comparison to the field. If the initial binary distribution would be log-normal, this would require wide binaries to be formed by other processes see for example Kouwenhoven et al. (2010); Moeckel & Bate (2010). However, apart from the wide binaries, the overall result does not seem to be very sensitive to the initial distribution. In our work a log-uniform period distribution as for the investigation of the orbital decay is applied. Otherwise the treatment is very similar to previous work.

The destruction of the wide binary systems is accompanied by a reduction of the binary frequency by  $13\% \pm 2\%$  after 3 Myr where the error is given by the standard deviation among the 50 realisations. However, this represents only a lower limit for the destruction of binaries by dynamical interactions. As has been mentioned before, although all stars are intended to be part of a binary initially, a certain fraction of all binaries - dominantly the wide - is 'disrupted' during the setup process. Treating these as being destroyed by the cluster dynamics results in an upper limit of  $26\% \pm 2\%$ . In summary, the effect of the dynamical destruction of wide binaries is a reduction of  $\approx 13\% - 26\%$  of the binary frequency during the first 3 Myr. Comparing this to the 12% loss of binaries by merger caused by orbital decay, this means that both processes are of equal importance, at least for the considered case.

In the following we specify the maximum effective period for the orbital decay  $P_{\text{orb}}$  and the minimum effective period for the dynamical destruction  $P_{\text{dyn}}$  at which at least 3% of the binaries are affected by the corresponding processes (see Fig. 6). The resulting values are  $P_{\text{orb}} = 5.5 \times 10^4$  days and  $P_{\text{dyn}} = 1.1 \times 10^5$  days, it follows  $P_{\text{orb}} < P_{\text{dyn}}$ . So there is no period range where both processes simultaneously play a role. Separating the two process as done here, does not take into account binaries that exchange partners and become more strongly bound. However, testing this for the here considered first 3 Myr of the cluster development, we found that only in  $\ll 1\%$  of all cases binary hardening leads to a transgression into the regime where orbital decay takes place. This means that both processes can be treated separately (see Fig. 6) in a additive way.

In order to determine the likelihood that our simulated period distributions correspond to the observed field population we performed  $\chi^2$ -tests as described by Press et al. (2007):

$$\chi^2 = \sum_{i=1}^N \frac{(R_i - S_i)^2}{R_i + S_i} \quad (9)$$

where  $N$  is the number of bins,  $R_i$  and  $S_i$  are the two distributions to be tested. This is only applicable if  $\sum_i R_i = \sum_i S_i$ . To warrant this we scaled our probability distributions to the total number of binaries observed by Raghavan et al. (2010). Afterwards the  $\chi^2$ -probability function  $Q(\chi^2|\nu)$  is used to calculate the probability that both distributions have been sampled from the same underlying distribution.

Table 2 shows the results of  $\chi^2$ -tests for the Raghavan et al. (2010) period distribution and the simulated one. Obviously, the probability that the initial period distribution and the observed period distribution of the field have been sampled from the same underlying distribution is negligible (probabilities of  $3.5 \times 10^{-7}$  and  $4.0 \times 10^{-3}$ ). Similarly, considering only one of the two processes "orbital decay" or "dynamical interaction" alone results in (higher, but still) low probabilities. Restricting the  $\chi^2$ -test to the proper period ranges ( $10^{-1} - 10^5$ d for the orbital decay and  $10^5 - 10^{10}$ d for the cluster dynamics) yields much better results - both the orbital decay and the cluster dynamics result in  $Q(\chi^2|\nu)$  values of 67% and 92%, respectively, indicating already the really good agreement of our simulated period distributions and the observations by Raghavan et al. (2010). A superposition of the distribution of periods  $P < 10^5$ d depleted by orbital decay and the distribution of periods  $P > 10^5$ d resulting from the dynamical destruction is shown as thick solid line in Fig. 7. Performing the  $\chi^2$ -test on this complete distribution over the entire period range results in a  $Q(\chi^2|\nu)$ -value of 94.1%. This clearly demonstrates, that together these two processes naturally reshape a log-uniform distribution to a log-normal distribution as observed in the field today.

	orbital decay		N-body dynamics	
	complete period range			
	$\chi^2$	$Q(\chi^2 \nu)$	$\chi^2$	$Q(\chi^2 \nu)$
initial	71.5	$2.3 \times 10^{-11}$	23.6	0.009
final	36.4	$7.2 \times 10^{-5}$	22.4	0.013
	adopted period ranges			
	$\chi^2$	$Q(\chi^2 \nu)$	$\chi^2$	$Q(\chi^2 \nu)$
initial	45.7	$1.1 \times 10^{-8}$	6.6	0.171
final	3.2	0.67	0.9	0.92

**Table 2.**  $\chi^2$ -test results calculated for the initial and final theoretical period distributions and those observed by Raghavan et al. (2010). The first four column block shows the results of tests against the complete Raghavan et al. (2010) period distribution ranging from  $\times 10^{-1} - \times 10^{10}$  d. The second four column block shows tests against the left part of the Raghavan et al. (2010) period distribution ( $\times 10^{-1} - \times 10^5$ d) for the orbital decay distributions and the right part of the Raghavan et al. (2010) period distribution ( $\times 10^5 - \times 10^{10}$ d)

## 5. Conclusions

In this paper we demonstrated for the first time that gas-induced orbital decay of binaries in the embedded cluster phase significantly changes the properties of short-period binary distribution. It turns out, this process is of equal importance for the development of the initial binary population as the well-studied process of dynamical evolution, at least for ONC-like clusters.

Gas-induced orbital decay not only changes the binary properties, but can even cause mergers of binaries, creating a more

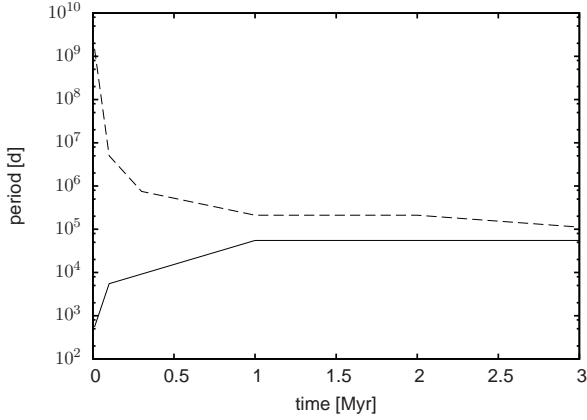


**Fig. 6.** Evolution of  $P_{\text{dyn}}$  (upper line) and  $P_{\text{orb}}$  in the first 3 Myr of cluster evolution.

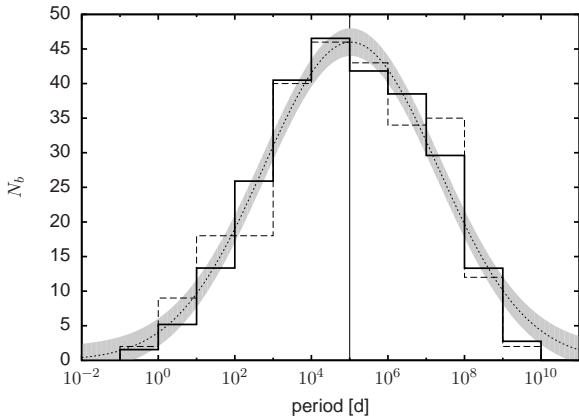


**Fig. 7.** Comparison of the period distributions resulting from the orbital decay of embedded binaries and the dynamical destruction (thick solid line) with the observations by Raghavan et al. (2010) (dashed line). Additionally, the log-normal fit by Raghavan et al. (2010) is shown as short-dashed line.

massive single star. The likelihood of such mergers depends on the density profile of the gas and on the separation and the mass of the binary system. For example, while binaries with semi-major axis of 10 AU rarely merge after 1 Myr in a cluster with a maximum gas density of  $10^5 \text{ cm}^{-3}$ , 40% of all binaries with a semi-major axis of 0.1 AU do so. In general the separation between binary systems with  $M_{\text{sys}} > 10 M_{\odot}$  shrinks on average to less than half its initial value after 1 Myr.

Orbital decay changes only the period distribution of short period binaries. However, long-period binaries, are affected by dynamical destruction caused by the interaction of the stars in a dense cluster environment. Our simulations show that intermediate period binaries are nearly unaffected by either of these two processes (see Fig. 8).

For an ONC-like cluster we found that for these G-type primary stars that the orbital decay due to the interaction of the binaries with the ambient gas basically only affects binaries with periods smaller than  $5 \times 10^4 \text{ d}$  corresponding to separations closer than  $\approx 36 \text{ AU}$ . By contrast, dynamical interactions destroy only binaries with periods larger than  $10^5 \text{ d}$  (i.e.  $\approx 53 \text{ AU}$ ). This means that there is no region in the period distribution that is influenced by both effects. Therefore it is possible to investigate the two processes separately and combine the results.

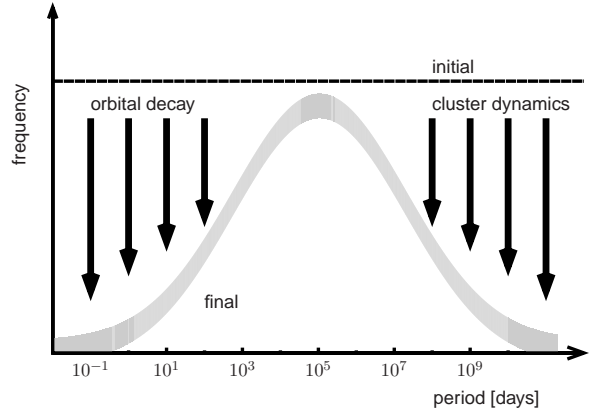


**Fig. 8.** Schematic illustration of the two-stage process forming the log-normal field-binary period distribution observed today (grey line) from an initial log-uniform distribution (solid line).

Perhaps the most striking result of this investigation is, that these two processes transform a primordial log-uniform into a log-normal period distribution, on a realistic time scale. The distribution resembles, in all its properties, remarkably that observed in the field, without need of further assumptions. Performing a  $\chi^2$ -test of the resulting distribution and recent observations of the field binary population (Raghavan et al. 2010) yields a probability of 94.1% that both distributions originate from the same origin.

The emerging picture can be summarized the following way (illustrated in Fig. 8): Binaries born in dense, embedded clusters with initially log-uniformly period distributions are processed in two ways. As long as the cluster is embedded in its natal gas (about 1 Myr), the orbital decay of the embedded binaries depopulates the left hand side of the period distribution. The dynamical evolution of the cluster destroys wide binaries, depopulating the right hand side of the period distribution. The combined effect of these equally important processes is that the final period distribution of the binary population in the star cluster has become log-normal although it initially has been log-uniform.

This re-shaping of the period distribution leads to a reduction of the binary frequency by 29%. The gas-induced orbital decay shrinks the separation between two stars such that mergers in 14% of all cases are possible. The dynamical interactions destroy 15% of G-type binaries by three-body encounters. This latter fraction only represents a lower limit to the reduction of the binary frequency due to our specific setup procedure and can be as high as 28%. Consequently the overall reduction of the binary frequency could be up to 42%. Assuming that most stars form in an ONC-like cluster and adopting a field binary frequency of G-type primaries is 58% (Raghavan et al. 2010) our results strongly favour a much higher initial binary frequency of 87% – 100% (assuming 44% one gets 73 – 86%) for solar-type stars.

Mass segregation and high densities in the cluster centre favour the merging of massive stars. From the merging of predominantly massive stars, one would expect to see a difference in the IMF of single and binary stars, with the single star distribution having an excess of massive stars. This has not been observed. However, the situation is more complex. Massive stars are as well the most likely to capture a new partner. For example mergers which form a stars with  $M > 20 M_{\odot}$ , can happen on a timescales of  $10^4 \text{ yr}$  (Pfalzner & Olczak 2007). The merger product and its companion would become part of the binary population again. So the IMF of the single and binary population

would be changed by merger processes. Whether they would be effected to the same degree would require further studies, but given the poor statistics at the high mass end, they would be indistinguishable.

Clearly, the field distribution is a mixture of stars originating from stars that experienced star formation in isolation, sparse (Taurus-like), dense (ONC-like) and very dense (Arches-like) clusters. On the one hand, associations like the Taurus clusters probably never had a gas density above  $10^4 \text{ cm}^{-3}$  and the current stellar density is below  $10 \text{ stars pc}^{-3}$  (Luhman et al. 2009). This means in such systems the binary population will neither be affected by orbital decay nor orbital destruction in a significant way and is therefore nearly unaltered from its primordial state. On the other hand, orbital decay becomes important for high gas densities and dynamical destruction for high stellar densities

On the basis of actual observations, one can only speculate how many stars are born in these different density regions. While Bressert et al. (2010) stated, that only a minor part of all stars in the solar neighbourhood form in high density regions, this is unclear for the total of the galaxy. Dukes & Krumholz (2011) concluded, that  $1/2 - 2/3$  of all stars are in clusters with more than 1000 stars. As such massive clusters initially had a much higher stellar densities (Pfalzner 2009), this indicates that environmental effects are important for the latter. The remarkable resemblance of the distribution, obtained after both processes have taken place, to the log-normal period distribution of the field binary population is a strong indication, that ONC-like clusters might be a dominant contributor to the field distribution.

Additional to the here studied ONC-type clusters, further investigations should include a variety of initial conditions: different stellar and gas density distributions (Kroupa 1995b; Parker et al. 2011), a range of cluster densities (Olczak et al. 2010; Marks et al. 2011) and different virial states of the cluster (Allison 2009). Currently we test the limitations of the model of orbital decay by numerical simulations (Kornreff & Pfalzner, in prep).

To verify our initial conditions observationally, detailed studies of binary populations in very young ( $< 100000 \text{ yrs}$ ) embedded star clusters, before the onset of the here investigated processes, would be necessary. However conclusions about the binary distribution in such young systems would be hindered by low-number statistics. Usually only a few tens of stars are observable, although the true membership might be considerably higher due to the high extinction in these clusters. Combining data from different such clusters would be an alternative. An other approach could be to observe different regions within a single OB associations. The processes are predominant at work in the association centre and much less so in the outskirts. Therefore, it could be expected that the period distribution in the association centre differs considerably from the outskirts - close to the log-normal in the cluster center and log-uniform in the outskirts. However, this picture neglects the mixing within the cluster, so that further theoretical work is needed to investigate this point.

*Acknowledgements.* We thank the referee for providing constructive comments and help in improving the contents of this paper and P. Kroupa for useful discussions on this topic. The simulations were performed at the Jülich Supercomputer Centre, Research Centre Jülich within Project HKU14.

## References

- Allison, R. J., Goodwin, S. P., Parker, R. J., et al. 2009, *ApJ*, 700, L99
- Binney, J. & Merrifield, M. 1998, *Galactic astronomy*, ed. Binney, J. & Merrifield, M.
- Binney, J. & Tremaine, S. 1987, *Galactic dynamics*, ed. Binney, J. & Tremaine, S.
- Bonnell, I. A. & Davies, M. B. 1998, *MNRAS*, 295, 691
- Bressert, E., Bastian, N., Gutermuth, R., et al. 2010, *ArXiv e-prints*
- Connelley, M. S., Reipurth, B., & Tokunaga, A. T. 2008, *AJ*, 135, 2526
- Dukes, D. & Krumholz, M. R. 2011, *ArXiv e-prints*
- Duquenois, A. & Mayor, M. 1991, *A&A*, 248, 485
- Fischer, D. A. & Marcy, G. W. 1992, *ApJ*, 396, 178
- Heggie, D. C. 1975, *MNRAS*, 173, 729
- Hillenbrand, L. A. 1997, *AJ*, 113, 1733
- Hillenbrand, L. A. & Hartmann, L. W. 1998, *ApJ*, 492, 540
- Jones, B. F. & Walker, M. F. 1988, *AJ*, 95, 1755
- Kaczmarek, T., Olczak, C., & Pfalzner, S. 2011, *A&A*, 528, A144+
- Köhler, R., Petr-Gotzens, M. G., McCaughrean, M. J., et al. 2006, *A&A*, 458, 461
- Kouwenhoven, M. B. N., Brown, A. G. A., Zwart, S. F. P., & Kaper, L. 2007, *Astronomy and Astrophysics*, 474, 77
- Kouwenhoven, M. B. N., Goodwin, S. P., Parker, R. J., et al. 2010, *MNRAS*, 404, 1835
- Kraus, A. L. & Hillenbrand, L. A. 2007, *ApJ*, 662, 413
- Kroupa, P. 1995a, *MNRAS*, 277, 1491
- Kroupa, P. 1995b, *MNRAS*, 277, 1522
- Kroupa, P. 2000, *New A*, 4, 615
- Kroupa, P. 2007, *ArXiv Astrophysics e-prints*
- Kroupa, P., Aarseth, S., & Hurley, J. 2001, *MNRAS*, 321, 699
- Kroupa, P. & Bouvier, J. 2003, *MNRAS*, 346, 343
- Kroupa, P. & Burkert, A. 2001, *ApJ*, 555, 945
- Lada, C. J. & Lada, E. A. 2003, *ARA&A*, 41, 57
- Luhman, K. L., Mamajek, E. E., Allen, P. R., & Cruz, K. L. 2009, *ApJ*, 703, 399
- Marks, M. & Kroupa, P. 2011, *ArXiv e-prints*
- Marks, M., Kroupa, P., & Oh, S. 2011, *ArXiv e-prints*
- Moeckel, N. & Bate, M. R. 2010, *MNRAS*, 404, 721
- O'Dell, C. R., Henney, W. J., Abel, N. P., Ferland, G. J., & Arthur, S. J. 2009, *AJ*, 137, 367
- Olczak, C., Pfalzner, S., & Eckart, A. 2010, *Astronomy and Astrophysics*, 509, 63
- Olczak, C., Pfalzner, S., & Eckart, A. 2010, *A&A*, 509, A63+
- Olczak, C., Spurzem, R., Henning, T., et al. 2011, *ArXiv e-prints*
- Padmanabhan, T. 2001, *Theoretical Astrophysics - Volume 2, Stars and Stellar Systems*
- Parker, R. J., Goodwin, S. P., & Allison, R. J. 2011, *ArXiv e-prints*
- Parker, R. J., Goodwin, S. P., Kroupa, P., & Kouwenhoven, M. B. N. 2009, *MNRAS*, 397, 1577
- Pfalzner, S. 2009, *A&A*, 498, L37
- Pfalzner, S. & Olczak, C. 2007, *A&A*, 475, 875
- Preibisch, T., Balega, Y., Hofmann, K., Weigelt, G., & Zinnecker, H. 1999, *New A*, 4, 531
- Press, W. H., Teukolsky, S. A., Vetterling, W. T., & Flannery, B. P. 2007, *Numerical Recipes 3rd Edition: The Art of Scientific Computing*, 3rd edn. (New York, NY, USA: Cambridge University Press)
- Prosser, C. F., Stauffer, J. R., Hartmann, L., et al. 1994, *ApJ*, 421, 517
- Raghavan, D., McAlister, H. A., Henry, T. J., et al. 2010, *ApJS*, 190, 1
- Reipurth, B., Guimarães, M. M., Connelley, M. S., & Bally, J. 2007, *AJ*, 134, 2272



Sridharan, T. K., Beuther, H., Saito, M., Wyrowski, F., &  
Schilke, P. 2005, *The Astrophysical Journal*, 634, L57  
Stahler, S. W. 2010, *MNRAS*, 402, 1758